

Structural behavior of reinforced soil walls under seismic loads

Reynaldo Melquiades Reyes Roque¹, Lincoln Jimmy Fernández Menacho¹,

Brayanm Reynaldo Reyes Huerta², Fabrizio del Carpio Delgado³

¹School of Civil Engineering, Faculty of Civil Engineering, Universidad Nacional Santiago Antúnez de Mayolo, Huaraz, Perú

²Department of Information Systems Engineering, Faculty of Engineering, Universidad Peruana de Ciencias Aplicadas, Lima, Perú

³School of Civil Engineering, Faculty of Engineering and Architecture, Universidad Nacional de Moquegua, Moquegua, Peru

Article Info

Article history:

Received Nov 4, 2024

Revised May 19, 2025

Accepted Jun 8, 2025

Keywords:

Deformations

Reinforced soil walls

Seismic load

Static state

Structural behavior

ABSTRACT

One of the main engineering challenges has been to design an economical soil retaining structure with high seismic resistance. From this perspective, reinforced soil walls have been developed with a focus on flexibility, in order to efficiently resist the effects of similar historical events in the event of a significant earthquake. The overall objective of this study was to compare the structural behavior of a geogrid-reinforced soil wall (Terramesh® system) under static and pseudo-static loads, and in a seismic environment simulated using the finite element method, in a shopping center in Trujillo, Peru. A case study was conducted using a mixed methodology, both applied and analytical-comparative in scope. Furthermore, the finite element methodology, material constitutive modeling, and dynamic time-history analysis of modal structures were chosen. It was determined that seismic loading can produce a 53.33% increase in deformations compared to the static state; Likewise, the overall safety factor under dynamic conditions tends to decrease by 27.85% compared to the static case. This study demonstrated the scope of geogrid reinforcement (Terramesh® system) through a practical case of a reinforced soil wall, using Plaxis 2D software to compare, estimate, and compare structural behavior in static, dynamic, and simulated environments.

This is an open access article under the [CC BY-SA](https://creativecommons.org/licenses/by-sa/4.0/) license.



Corresponding Author:

Reynaldo Melquiades Reyes Roque

School of Civil Engineering, Faculty of Civil Engineering, Universidad Nacional Santiago Antúnez de Mayolo

Huaraz 02002, Perú

Email: rreyesr@unasam.edu.pe

1. INTRODUCTION

Structural behavior is the reaction or response of a construction, regardless of the materials it is made of, to an external action produced by a given force [1]. This response is associated with indicators such as stiffness, strength, and ductility [2]. Similarly, the estimation of the degree of response that the structure generates to high seismic loads is carried out through experimental tests under both dynamic and static environments [3]. Therefore, various structures, such as walls and the like, must be designed to demonstrate sufficient strength and ductility to ensure overall safety under seismic forces [4].

Since Peru is one of the most seismically active countries in the world, it is evident the a need to use simplified methods or advanced numerical analysis of computational type to analyze the structural behavior, taking into account the finite element method [5]. This is in order to assess this type of response, according to the deformations generated in the constructions under eventualities and potential events [6]. However, in conditions under dynamic loads, the analysis of these deformations allows the evaluation of the behavior of the structure under dynamic loads [7], [8].

In the present study, a geogrid-reinforced soil wall was analyzed according to the Terramesh® system [9]. It is composed of pre-assembled double-twisted wire mesh units (type 8×10) as shown in Figure 1. It is a structure almost 17 m high and a total area of 388 m², located in an area that is considered critical because it is located in a commercial center of the city of Trujillo, on the right bank of the Santa River, twenty minutes from the center of the city of Huaraz in Peru as shown in Figure 2. It should be noted that the walls designed under the Terramesh® system are characterized by having a double-twisted hexagonal steel mesh, placed horizontally on the slope, slightly stepped, and coated with a compact mix on the surface [10], [11].



Figure 1. Side view of reinforced soil wall under the Terramesh® system



Figure 2. Plan view of the location of the reinforced soil wall under the Terramesh system®

This wall was designed as a containment mechanism for the backfill soil for different steel and reinforced concrete structures with foundations. These structures function as storage for food products (permanent dead loads) and receive trailer loads (transitory live loads). The design was based on the recommendations of the manufacturer, Maccaferri, using Macstars software, developed with the limit equilibrium method. Verification of internal and external stability was contemplated, as well as global stability for static and pseudo-static conditions. However, these pseudo-static stability verifications do not provide any information on the deformations in the wall caused by seismic action.

In a related context, earlier studies have explored aspects that align with the current research. For instance, Xu *et al.* [12] examined the seismic stability and behavior of reinforced soil walls through shaking table experiments. They emphasized that accounting for higher acceleration amplification in the upper portion of the reinforced wall, as well as the phase difference between peak lateral earth pressure and the inertial force acting on the backfill, can lead to more precise predictions.

Similarly, Lin *et al.* [13] investigated the mechanical response of a flexible geogrid-reinforced soil wall under dynamic loading conditions. They noted that the wall's dynamic deformation behavior is influenced by factors such as the number of vibration cycles, the amplitude of the dynamic load, and the frequency of the vibrations. As the load amplitude increases, dynamic deformation becomes more pronounced, and after a cumulative vibration of 200×10^{-1} times, both the lateral and vertical deformation ratios of the wall face remain under 1%.

On the other hand, Hamdi *et al.* [14] studied the settlement of the sandy fill soil behind the retaining wall under dynamic loads, with respect to the factor of safety (FoS), and as the load increases from 0 kPa to 100 kPa, the magnitude of the safety factor decreases. Furthermore, it is noted that the geogrid-reinforced soil retaining wall is unstable when load increases exceed 90 kPa. The safety factor required for reinforcement stability should be equal to 1.5.

Within the same framework, Johari and Maroufi [15] conducted a reliability analysis of a geogrid-reinforced retaining wall system using the random finite element method. The objective was to assess lateral displacement, calculated as the ratio between the allowable lateral displacement and the wall's maximum observed displacement. The study concluded that the FoS is influenced by the positioning of the geogrid; specifically, the likelihood of failure increases as the geogrid is located nearer to the top of the wall. In a related study, Lu *et al.* [16] examined the seismic performance of a steel structure outfitted with precast external walls and a newly designed connection system. Numerical simulations using ABAQUS were employed to analyze the behavior of both the precast walls and the innovative connections. The results demonstrated that the inclusion of precast external walls and the new connection design affects the seismic response of the steel structure. Additionally, increasing the prestressing force of the top joint bolts was found to have only a minor effect, slightly improving the stress distribution in both the steel frame and the connection joints.

Finally, Akbar *et al.* [17] analyzed the seismic performance based on the displacement of earth retaining walls with geogrids using three-dimensional finite element modeling. Based on the above, this

study highlights the importance of computational finite element modeling to determine the feasibility of using geogrids (Terramesh® system) as reinforcement for retaining structures in a simulated seismic environment. These studies evidently addressed similar problems, involving geogrid-reinforced walls or structures, and resorted to simulation using finite element computational models. However, a comparative analysis of behavior in environments with static and dynamic loads, as well as in simulated environments in the same space and time, was lacking. Furthermore, these studies specifically reference the Terramesh® system, which is identified as a research gap addressed in this study. To address this gap, this study proposes a novel approach using computational modeling using Plaxis 2D V16 software. Seismosoft software is also used, supported by Microsoft Excel, for data processing and obtaining structural responses.

Therefore, the overall objective of this study was to compare the structural behavior of a geogrid-reinforced soil wall (Terramesh® system) under static, pseudo-static, and finite element-simulated seismic loads. The specific objectives were to determine the variation in the lateral displacement produced by the seismic load compared to the lateral displacement under static conditions in the Terramesh® reinforced soil wall of a shopping center in Trujillo. Subsequently, the variation in the settlement produced by the seismic load compared to the settlement under static conditions in the Terramesh® reinforced soil wall of a shopping center in Trujillo was determined.

Finally, the variation in the safety factor calculated in the presence of the load was specified. Consequently, the development of this study and the results obtained demonstrate that advances in physical and mathematical modeling techniques, technology, and the increased capacity of computerized equipment have opened up a field for the improvement of analytical techniques, particularly the development of refinement and improvement of the finite element method. Through these methods, it is possible to resolve critical situations associated with geotechnical and seismic engineering by applying advanced material constitutive models and the effects of earthquake-induced pore pressure, considering specific cases of any type of structure.

2. RESEARCH METHOD

This research was developed under the mixed research approach [18], considering a case study [19], with a non-experimental and observational design [20] of analytical-comparative scope [21]. Similarly, a model was developed through the application of Plaxis 2D V16 software, in addition to Seismosoft, with the support of Microsoft Excel for data processing and obtaining structural responses. It was carried out in two environments, both in the static and dynamic states, to then compare and analyze the discrepancies and similarities. It should be noted that, technically, this is a study framed within the guidelines of geotechnical engineering, static and dynamic structural analysis, and numerical analysis with finite elements. In this sense, a methodology is proposed to analyze the application of a seismic load on the structural behavior of the soil wall reinforced with the Terramesh® system.

2.1. Materials

The study had the following working materials and resources: a record of information as an instrument of direct observation, which served as a basis for ordering and tabulating the information obtained and performing the statistical analysis [22]. Technical building standard E030. Earthquake-resistant design [23]. Plaxis 2D V16 software for data processing and obtaining the structural response. This software is capable of developing a numerical matrix analysis using the finite element method [24]. SeismoSignal V.2022 software for the correction of accelerograms [25]. SeismoMatch V.2022 software [26] to make the acceleration records compatible with the design spectrum of the E030 standard, which has a return period of 475 years, and accelerographic records [27].

2.2. Methods

The technical study included the following methods: computational modeling [28], methodology based on finite element method analysis [29], dynamic analysis of time-history modal structures [30], comparative method considering the results of the findings without seismic load (O1) and the results with seismic load (O2) obtained from the reinforced soil wall as a sample of the study. This establishes two possible panoramas, one in a static state and the second in dynamic conditions.

2.2.1. Work procedure

The work procedure is divided into six (6) phases that develop the following activities: i) characterization of the site and structural arrangement of the Terramesh® system adapted to reality, ii) tectonics and seismology, iii) calibration of models in finite element method software, iv) static operational analysis of the Terramesh® wall, v) dynamic analysis of the Terramesh® wall, and finally, vi) determine the

impact on structural behavior. Likewise, it contains the activities, elements, specifications, and observations. The limitations and critical situations that justify the selection of this protocol are also specified.

With the processing of the data by means of the aforementioned software, the specific details for the computerized modeling were formed. Once the parameters of the reinforced soil wall under study were obtained, the computational modeling of the wall was developed using Plaxis 2D V16 software. For this purpose, access was sought by applying the static and dynamic stresses, considering the construction phases. Strategic points were located in the modeling to estimate the value of the results of each of these, and thus present the diagnostic situation of the structural behavior.

Likewise, the finite element model was calibrated with the Plaxis 2D V16 software and the specifications of the wall reinforced with the Terramesh® system. In addition, for the processing of the synthetic accelerograms, Seismosoft was used, specifically, SeismoSignal V.2022 for the correction of accelerograms. SeismoMatch V.2022 was used to make the records compatible with the design spectrum of the E030 standard, which has a return period of 475 years.

3. RESULTS AND DISCUSSION

3.1. Calibration of the modeling for the study

Updated information on geometry, definition of soil strata properties, definition of reinforcement element properties, and boundary conditions was collected and arranged in the foreground for modeling in Plaxis 2D V16. This allowed the simulation of the upper structures through the loads applied to the model, the definition of the movement of the base of the model (accelerographic record) by means of a prescribed displacement, the creation of the finite element mesh, the definition of the water table and the simulation of the construction process of the wall under the Terramesh® system. The records of the earthquakes in Huacho (17-10-1966), Ancash (31-05-1970), and Lima (03-10-1974) were considered with the information shown in Table 1.

Table 1. Seismic records considered for the study

Seism	Name	Localization		Depth.	Size	Peak	Name	Comp.	Code
		Lat.	Long.	(Km)	(Mw)	acceleration (G)			
Huacho (17-10-66)	PQR	-10.7°	-78.7°	24	8.1	0.40	N82W	Horiz.	7035
							NO8E	Horiz.	7036
Ancash (31-05-70)	PQR	-9.36	-78.87	64	7.9	0.10	-	Horiz.	7038
							-	Horiz.	7039
Lima (03-10-74)	SCO	-12.28°	-77.54	21.2	8.2	0.26	1421 GCT NO8E	Horiz.	7050
							1421 GCT N82W	Horiz.	7051

3.2. Corrections to the available accelerograms used

In order to achieve a reliable approximation of the acceleration data recorded during an earthquake at the site, a careful treatment of the available records was carried out. This is due to the fact that the information collected in the field is in the original format of the accelerograph. The corrections are of instrumental order, on the quadratic baseline and filter corrections, which were processed using the SeismoSignal software. The accelerographic records in both directions, corrected in SeismoSignal, of the 1966 earthquake are shown in Figure 3, the 1970 earthquake is shown in Figure 4, and the 1974 earthquake is shown in Figure 5. The records were obtained from SeismoSignal, with N-S representing the horizontal direction north-south and E-W representing the horizontal direction east-west.

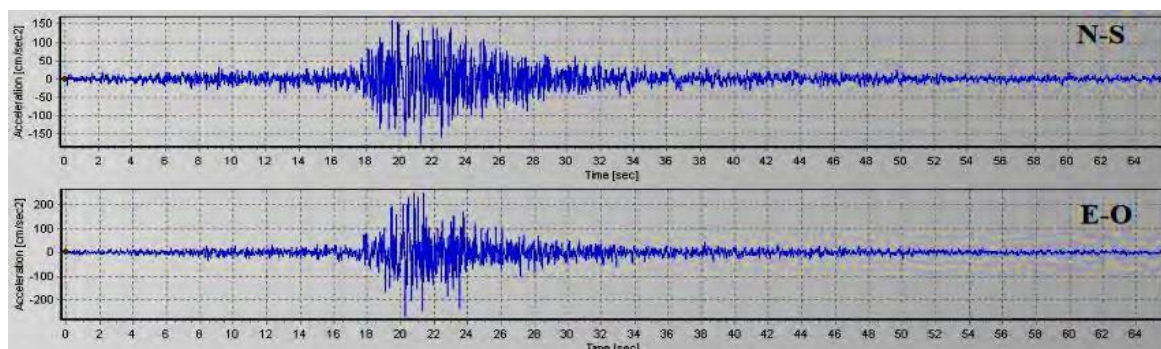


Figure 3. Record of corrected accelerations of the Huacho earthquake, October 17, 1966

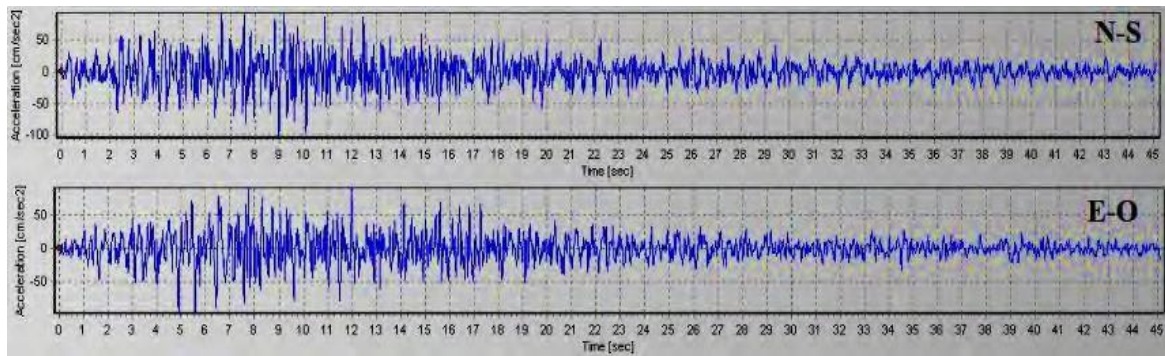


Figure 4. Corrected acceleration record of the Ancash earthquake, May 31, 1970

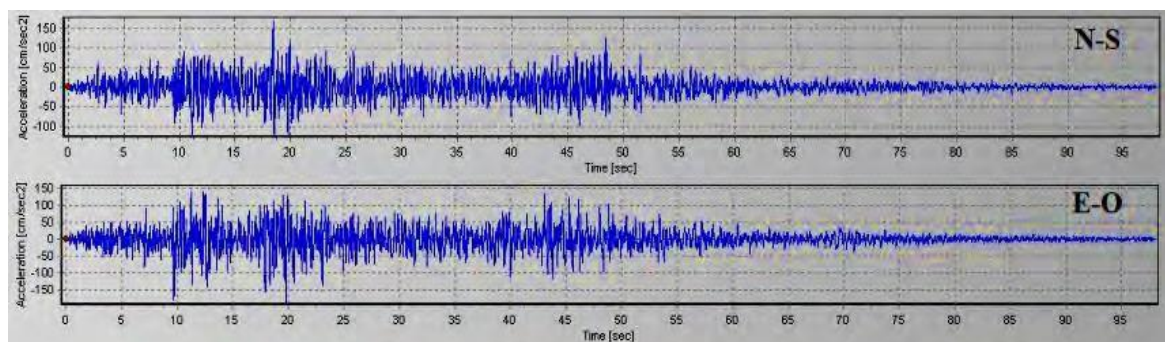


Figure 5. Corrected acceleration record of the Lima earthquake, October 3, 1974

For the analysis, the east-west and north-south records of 3 seismic events recorded by the accelerographic network of the Centro Peruano Japonés de Investigaciones Sísmicas y Mitigación de Desastres (CISMID) of the Faculty of Civil Engineering of the National University of Engineering were processed. Likewise, information on the parameters of the strata associated with the soil was compiled. This information is shown in Table 2.

Table 2. Parameters of the soil strata considered for the study

Parameter	Reference	0-Deep layer	1-Bedroc 2-Clay saprolitek	2-Clay saprolitek	3-Backfill affirmed	4-Filling classified buttons	5-Terramesh® system	Und.
Constitutive model	Model	MC	HS	HS	HS	MC	MC	-
Drainage type	Type	Drained	Not drained	Not drained	Drained	Drained	Drained	-
Weight of soil unit above	γ	23	20	17.64	20	19.15	18	kN/m ³
Weight of soil unit above	γ	23	20	17.64	20	19.15	18	kN/m ³
Initial void ratio	e_{init}	0.30	0.40	0.45	0.5	0.6	0.45	-
Strength parameters								
Secant stiffness in a standard drained triaxial test	$_{ref} E$	150000	100000	59000	60000	50000	120000	kN/m ²
Tangent stiffness for primary oedometer loading	$_{ref} E$	-	100000	59000	60000	-	-	kN/m ²
Unloading/reloading stiffness	E^{ref}	-	300000	117000	180000	-	-	kN/m ²
Power for stress level stiffness dependence	m	-	0.9	0.85	0.75	-	-	-
Cohesion	c'	500.00	15.00	3.70	1.95	0.00	50.00	kN/m ²
Angle of friction	ϕ'	42.00	35.00	29.12	39.00	40.60	40.00	°
Angle of dilatancy	ψ	12.00	5.00	0.10	9.00	10.60	10.00	°
Poisson's ratio	ν'	0.35	0.30	0.30	0.30	0.20	0.35	-

3.3. Estimation of loads supported by the wall

3.3.1. Distributed loads

Normalized loads were introduced into the 2D model for a 1.00 m wide strip. First, the loads associated with the warehouse's steel structure, such as the self-supporting selective racking, were considered. These were composed of: dead load (DL), pallet load (PL), vertical impact loads per operation (IL), live load of the roof (Lr), the load due to pseudo-static seismic action (El), and the loads due to wind action (WL). Six (6) combinations were formed with respect to their location within the structure. Depending on their magnitude, the LRFD-COMB 2 arrangement, composed of 1.2 DL+1.4 PL+0.5 Lr, was chosen for the static loads on the self-supporting selective racking. Therefore, $4.31 \text{ tn/m}^2 = 43.1 \text{ kN/m}^2$ is considered, so for a 1 m wide strip, 43.1 kN/m^2 is required. The total load (TL) of the steel structure of the front warehouse (pipe warehouse) is then estimated, specifying the different loads, such as the DL and the live load (LL) of the frames. The LL per unit area is estimated, the ultimate load is calculated, and the load envelope is shown. TL of the pipe shed:

$$DL = 20 + 10 = 30 \text{ kg/m}^2$$

$$DL = 0.03 \text{ tn/m}^2 = 0.3 \text{ kN/m}^2$$

$$CV = 30 + 30.94 = 60.94 \text{ kg/m}^2 = 0.6094 \text{ kN/m}^2, \text{ then:}$$

$$CT = 1.4 CM + 1.7 CV \quad (1)$$

$$CT = 0.42 + 1.036 = 1.46 \text{ kN/m}^2$$

$$Envelope = 461.3 \text{ kg/m}^2 = 4.613 \text{ kN/m}^2$$

$$1.46 + 4.613 = 6.013 \text{ kN/m}^2, \text{ for a 1 m wide strip: } 6.01 \text{ kN/m}^2.$$

Load on reinforced pavement slab, marshalling yard, slab thickness of 0.20 m with reinforced concrete. Concrete weight= $2400 \text{ kg/m}^3 = 24 \text{ kN/m}^3$. Weight per slab thickness= $24 \times 0.20 = 4.8 \text{ kN/m}^2$, for a 1 m wide strip, this is equivalent to 4.80 kN/m^2 .

Other loads to consider are the pavement loads in the marshalling yard, the transient LL, and the operating load. For the reinforced pavement slab in the marshalling yard, it was found that for a 1 m wide strip, it is equivalent to 4.80 kN/m^3 . For the transient LL, the normalized load for a 1 m wide strip was determined to be equivalent to 8.90 kN/m^2 . Regarding the operating load, as specified in Standard E020 of the National Building Regulations, the minimum distributed LL for storage is 5.00 kPa, which, for a 1 m wide strip, is equivalent to 5.00 kN/m . The total values obtained and the total distributed loads were 67.81 kN/m . Point loads are determined by the perimeter fence. Considering a length of 1 m: Reinforce concrete foundation: $0.6 \times 0.6 \times 1 \text{ m} = 0.3 \text{ m}^3 \times 24 \text{ kN/m}^3 = 8.64 \text{ kN}$. Masonry wall: $3.2 \times 0.15 \times 1 \text{ m} = 0.48 \text{ m}^3 \times 18 \text{ kN/m}^3 = 8.64 \text{ kN}$. Confinement beam: $2 \times (0.3 \times 0.25 \times 1 \text{ m}) = 0.15 \text{ m}^3 \times 24 \text{ kN/m}^3 = 3.6 \text{ kN}$. Total weight of the perimeter fence: 20.88 kN . Table 3 shows a summary of the values obtained.

Table 3. Totalization of the estimated loads

Estimated loads	Value	Units
Self-supporting selective rack	43.10	kN/m
Nave tubest	6.01	kN/m
Pavement of the maneuvering yard	4.80	kN/m
Transient load	8.90	kN/m
Operational load	5.00	kN/m
Total distributed loads	67.81	kN/m
Perimeter fence	20.88	kN
Total point charges	20.88	kN

3.4. Geometry of the model for the study

Since the Plaxis 2D V16 software was used, the planar deformation model used for geometries with a section perpendicular to the x-y plane is more or less uniform, and a state of stress and symmetrical load distribution known as the radial symmetry model was chosen. This generates the discretization of the soils or structures, by means of triangular finite elements made up of 6 or 15 nodes, at places where the displacements will be measured. The geometry of the model is formed by the cross-section of the critical zone of the Terramesh® wall, which is 17 meters high. In this sense, the modeling of the critical section in the software involves the following: i) boundary conditions, ii) soil layers, iii) loads, and iv) reinforcement elements (movable supports).

For the static case, the analysis of deformations and safety factor was carried out at the end of the construction phases of the 17.00 m high wall under the Terramesh® system, with the construction of the

walkway at the foot of the wall. Next, the operational phase was introduced, in which the operational loads were applied to finally calculate the deformations and the safety factor in the operational loads phase. This analysis was performed at a global level considering the critical section of the wall. In this aspect, the Plaxis 2D software considers the conditions of terrain geometry, slope, geotechnical characteristics, soil strata, as well as the structural characteristics of the reinforcements that make up the Terramesh®.

At the lateral limits of the model, movable supports were considered, allowing vertical displacement and restricting the horizontal displacement of the nodes. A perfect embedment has also been considered at the base due to the high stiffness of the deep stratum. Figure 6 shows the model generated by the software, showing the finite element mesh composed of 5,627 elements and 46,054 nodes.

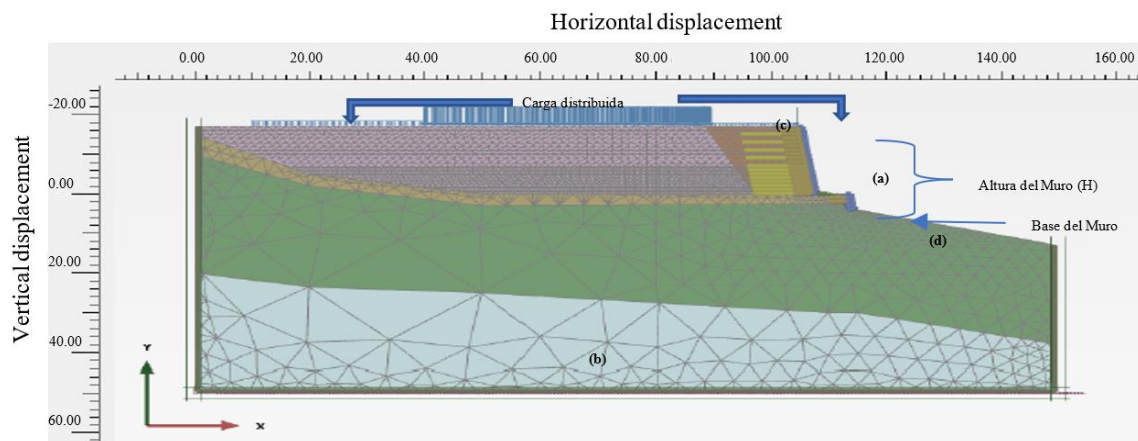


Figure 6. Finite element mesh for the study of the Terramesh® wall

3.5. Structural behavior of the Terramesh® wall under seismic loads

In the dynamic case, the deformation analysis and FoS were calculated from the seismic signals entered into the program, with a time interval of the dynamic substep (δt) that is equal to the time interval used in the input signal. All this is reflected in (2).

$$\delta t = \Delta t / (m \times n) \quad (2)$$

Where Δt is the time interval specified for the relevant phase (duration of the seismic event), m is the number of additional steps, and n is the number of dynamic substeps. The accelerographic records used in the investigation have a time interval of 0.20 seconds. To perform the dynamic calculation by steps, it was chosen to use the time interval close to where the maximum acceleration occurs; for this reason, an attempt was made to simplify the finite element model to speed up the calculation. Thus, using the recommended formula, the dynamic parameters shown in Table 4 were obtained.

Table 4. Calculation of dynamic parameters for the time interval of 0.20 sec

Dynamic parameters	Earthquakes			
	7035-7036	038-7039	7050-7051	Artificial
Δt	25	10	20	10
m	250	100	100	100
n	5	5	10	5

After applying the steps of the structured methodology following the use of the Plaxis 2D program, the results of the structural response obtained from the modeling of the wall reinforced with the Terramesh® system are shown. The observations were sectioned considering 9 specific points located at strategic sites that were generated by the program algorithm. The results were recorded in two moments, sectioned into static and dynamic domains. In the first one, the values were recorded for the post-construction operational state of the wall, and the estimates for earthquakes S. 7035, 7036, and 7038. In the dynamic case, the values associated with earthquakes S. 7039, 7050, and 7051 were handled. To complete the values, the results of the artificial earthquake were presented. The control points are specified in Table 5.

Table 5. Control points A-B-C

Item	Nodo	Coordinate	
		X	Y
A'	27670	85.00	17.00
A (médium)	33623	93.50	17.00
A	45980	105.60	17.00
B'	25034	85.00	8.00
B (médium)	39722	96.00	8.00
B	42223	107.00	8.00
C'	22504	85.00	0.00
C (médium)	28094	96.50	0.00
C	32438	108.00	0.00

3.5.1. Deformation analysis ($|U|$) and lateral displacements (U_x)

For the precise illustration and tabulation of the results achieved in each case, a section A-B-C was established where the points X: (105.60; 17.00) and X' (108.00; 0.00), which are located on the Terramesh® wall screen, are joined. Due to the number of nodes, only three points were considered in this section for the comparative analysis in terms of the effect generated in the static and dynamic states. One point was specified at a height of 0.00 m, one at 8.00 m, and one at 17.00 m in reference to the axis. The largest deformation in the static state is seen at point B, in S. 7038, with a $|U|=1.162$ m, while when subjected to dynamic loading, the result increases at the same point to a value of 1.683 m for S-7050. However, in the S. Artificial. Artificial dynamic case, at point B, the largest deformation was obtained with a value of 1.788 m. In general, it can be stated that for S. Artificial, points A, B, and C show the greatest deformation when facing dynamic loads, which is close to the behavior generated by S. Artificial for the dynamic case. Lateral displacement (U_x). For this analysis, three reference points were set within the network located at three nodes: A-B-C, as specified in Table 6. Table 6, point B, shows the highest values of deformation and lateral displacement. It is observed that the highest value of $|U|$ is observed in S. 7038 in the dynamic range of S. 7051, with 1683 m. Surpassed by the S. Artificial (1788 m). For displacement, the dynamic U_x was 1591 m for S. 7051, surpassed by the S. Artificial (dynamic), which presents a result of U_x of 1723 m.

Table 6. Deformations in meters (m) and lateral displacements generated in section A-B-C

Solicitation	Case	A	B	C	Case	A	B	C
		(105.60, 17.00)	(107.00, 8.00)	(108.00, 0.0)		(105.60, 17.00)	(107.00, 8.00)	(108.00, 0.0)
E. Operational	U (static)	0.551	0.658	0.528	U_x (static)	0.551	0.658	0.528
S. 7035		0.999	1.071	0.899		0.999	1.071	0.899
S. 7036		0.823	0.878	0.704		0.823	0.878	0.704
S. 7038	U (dynamic)	1.108	1.162	0.968	U_x (dynamic)	1.108	1.162	0.968
S. 7039		1.191	1.242	1.045		1.191	1.242	1.045
S. 7050		1.448	1.481	1.251		1.448	1.481	1.251
S. 7051		1.662	1.683	1.414		1.662	1.683	1.414
S. Artificial		1.784	1.788	1.536		1.784	1.788	1.536

3.5.2. Settlement analysis

The analysis of the structural response according to settlement (U_y) was carried out horizontally, considering three reference levels: A-A', B-B', and C-C'. Reference level A-A' covers the coordinates (85.0; 17.0), (93.50; 17.0), and (105.6; 17.0), reference level B-B' the coordinates (85.0; 8.0), (96.0; 8.0), and (107.0; 8.0), and reference level C-C' the coordinates (85.0; 0.0), (96.50; 0.0), and (108.0; 0.0). Table 7 shows the notable values according to the results achieved with the applied methodology.

Table 7. The results achieved for each level established in the study

Case	Solicitation	A (medium)	B (medium)	C
		(105.60; 17.0),	107.0; 8.0	96.50, 0.0
Uy (static)	E. Operational	-0.486	-0.315	-0.368
	S. 7035	-0.615	-0.439	-0.358
	S. 7036	-0.521	-0.358	-0.314
	S. 7038	-0.645	-0.437	-0.378
Uy (dynamic)	S. 7039	-0.678	-0.474	-0.392
	S. 7050	-0.745	-0.505	-0.428
	S. 7051	-0.885	-0.633	-0.521
	S. Artificial	-0.764	-0.515	-0.458

Table 7 shows that the highest settlement in absolute value is generated at point A (middle) for the dynamic tension case S. 7051 at a height of 17 M, that is, at surface level, for the static case at S. 7030, in the dynamic scope for S. 7051, exceeding the S. Artificial. This allows us to infer that the greater the seismic load, the greater the settlement at the highest point of the coordinates in both x and y. Considering the observation according to S, this may be associated with the fact that the greater the depth, the more compacted the soil at the site. Likewise, the force exerted by the static load in an environment similar to an 8.2 Mw earthquake may lead to greater settlement.

3.5.3. Factor of safety

For the determination of FoS, which represents the resistance capacity of the structure above the design load, the Phi-C reduction method of resistance reduction was chosen, developed using Plaxis software [31]. This is applicable when additional deformations are generated that have no relevant physical significance. But when reaching a stable value for the summation of the magnitude scale factors (ΣMsf), it allows to obtain the possible failure mechanism of the structure.

In the pseudo-static approach, a lateral force acting through the center of the sliding mass is applied, which generally proceeds in the off-slope direction that occurs depending on the design of the structure. With the use of Plaxis 2D in the finite element method, the stability of retaining structures, as in the case of this study, is estimated. For this purpose, the definition of failure, similar to the limit equilibrium method, is used. For this case, the Phi-C reduction method is used, where the shear strength parameters are reduced until they reach the rupture level. In this case, the FoS is calculated from the (3).

$$FoS = (\text{available force} / \text{Failure of force}) = \text{Value of } \Sigma Msf \text{ in case of failure} \quad (3)$$

However, it should not be forgotten that the network is very important in order to correctly determine the migrant occurring in the structure. An important point here is that the calculations can be performed in the gravity, plastic, consolidation, and safety load calculation options by entering the value specified in the pseudo-static option in the Plaxis 2D finite element program. In that sense, the FoS was estimated by means of the data entered in the software, associated with the value of the deformations $|u|(m)$ and the summation of the ΣMsf . This was performed after an energy dissipation phase, because the software does not allow for interlacing a calculation phase of this factor, after a dynamic calculation phase. Table 8 shows the results of the FoS.

Table 8. Consolidated values under the stability of the FoS for each stress

Case	Solicitation	FoS
FoS (static)	E. Operational	2.178
	S. 7035	1.183
	S. 7036	1.408
	S. 7038	1.205
FoS (dynamic)	S. 7039	1.211
	S. 7050	1.254
	S. 7051	1.325
	S. Artificial	1.187

3.5.4. Action of seismic loads on deformations, lateral displacement, and factor of safety

In order to have greater consistency in the findings presented, we proceeded to verify the premises, in which the structural behavior of the reinforced soil wall is associated with the loads in static, semi-static, and dynamic environments (including simulated seismic environments). With the collected historical data, normality tests were performed using the Shapiro-Wilk line. Here, it was found that they do not follow a behavior similar to a normal distribution. Due to this, the application of the T-student test was chosen to verify that the difference of the means of the deformations of the dimensions, lateral displacement, settlements, and safety factor in the considered environments generates a positive value. Table 9 shows the results obtained.

In the case of the general premise, it corresponds to the response of the general objective of the study. This shows that the difference of means was different from zero and of positive value, which is interpreted as a significant effect of the seismic load on the increase of the wall deformation. The same effect is seen for the lateral displacement from inside to outside, from left to right. As for the settlement, although this is of smaller value in terms of the difference, it can be seen that the seismic load has a significantly small effect. In relation to the safety factor, a difference with a negative value (-0.345) was observed; this allows inferring that as the seismic load increases, this factor is reduced, exposing the system to potential structural

damage, thus requiring an effective and efficient reinforcement system. In comparison to the values generated in dynamic and simulated mode, the maximum values obtained were considered for comparison and, in this way, to determine the degree of estimation performed by means of the Plaxis 2D software. Table 10 shows the results obtained. The values in Table 10 indicate that using the applied procedure, the values of deformation and lateral displacement can be estimated using S. Artificial, achieving a significantly acceptable estimate.

Table 9. Results of the average in each dimension of structural performance under both static and dynamic conditions

Structural performance dimensions	Media (μ)			
	E. Dynamic	E. Static	Variation ($\Delta\mu$)	Variation (%)
Deformations ($ U $)	1.245 m	0.577 m	0.664 m	53.33
Lateral displacement (U_x)	1.168 m	0.394 m	0.773 m	66.18
Settlements (U_y)	0.361 m	0.272 m	0.091 m	25.20
Factor of safety (FoS)	1.238	1.586	-0.345	-27.86

Table 10. Variation of values with respect to deformation, lateral displacement, settlements, and FoS

Structural performance dimensions	Maximum value			
	E. Dynamic	S. Artificial	Variation	Variation (%)
Deformations ($ U $)	1.683	1.778	-0.095	-5.34
Lateral displacement (U_x)	1.591	1.723	-0.132	-7.66
Settlements (U_y)	0.745	0.885	-0.140	-15.89
Safety factor (FoS)	1.325	1.187	0.138	10.41

3.6. Discussion

Overall, the findings highlighted the importance of applying computer models to the study of finite element structural behavior in geogrid-reinforced wall structures. Thus, a significant effect of seismic loading on increasing wall deformation was recorded. The same effect is observed for lateral displacement from inside to outside, from left to right. Regarding settlement, although it is of smaller value in terms of difference, it can be observed that seismic loading has a significantly small effect. This result aligns with the contributions generated by [32], who stated that as the amplitude of the dynamic load increases, the development of dynamic deformation gradually increases.

Considering the values obtained associated with wall deformation due to seismic loads, it tends to be greatest at the midpoint of the wall's height (H). This is associated with the displacement in the X-X direction, which increases at the midpoint of the critical zone located at coordinates (95.00, 8.00). Likewise, it was shown that it is most intensely observed in $\frac{1}{2} H$ of the wall in the dynamic domain, as in an artificial seismic system. This is consistent with the results of [33], who observed that when greater ground acceleration is generated, horizontal displacement (from inside to outside) in the direction of the wall's location increases. This directly influences wall deformation, with a greater presence in the upper middle part of the wall. Therefore, there is a need to improve wall reinforcement at the top to avoid undesirable consequences, considering the observations and findings noted.

Regarding variable ground settlement (vertical displacement Y-Y), the results show that the greatest settlement in absolute value occurs at the midpoint of the critical zone, at the surface level, at a height of 17 m above the base of the wall. Regarding settlements, an increase of 0.091 m was determined, produced by the seismic load, compared to the settlement under static conditions. It is important to note that this variation decreases as the wall base is approached. This finding is consistent with the results and contributions of [34], who indicated that ground settlement decreases as the relative density decreases, due to the soil's more stable nature. Therefore, it can be observed that the settlement decreases at greater depths. These results suggest that the geogrid system for a wall of these characteristics could present certain disadvantages compared to other reinforcement methods. Regarding the FoS, it was determined that, in operational conditions, the estimated value was the highest. This is because the dynamic loads are relatively low, so the seismic hazard coefficient (SRC) tends to be lower. Conversely, as the seismic load progressively increases, the FoS decreases because the available force/failure force ratio progressively decreases. This is consistent with [35], who stated that as the load increases from 0 kPa to 100 kPa, the magnitude of the safety factor decreases.

Based on the results, the importance of computational modeling using the finite element method was assessed. A logical sequence was observed, presenting, first, geometric modeling, finite element modeling, definition of the environment to be simulated, and the analysis and corroboration of the results. This approach is supported by the contributions of [36]. The former achieved the objectives of their study through

numerical simulation with the ABAQUS software package to further investigate the performance of the precast exterior wall and the proposed new connection methods. The latter, through three-dimensional finite element modeling.

As a limitation, it should be noted that in this work, a case study was modeled using Plaxis 2D, which uses different numerical approaches. Although this software allows for the simulation of soil deformation and takes into account soil-structure interaction, other resources have been applied in various studies to simulate soil stiffness. They can also include an iterative procedure to adjust the ground pressure based on wall deformation.

However, one notable property of Plaxis 2D is that it allows for the accurate assessment of structural displacement, such as reinforced walls at the top of the wall. However, it is important to highlight that Plaxis 2D was developed based on Plaxis 3D, which has already been tested in similar studies for tunnels and foundations. It has demonstrated better performance than Plaxis 2D in predicting displacements. Based on the above, it is recommended that future research involving the use of a computational model should conduct an in-depth review of new trends in simulation models that can be applied to structural behavior studies in both dynamic and static environments. This is expected to result in more efficient performance.

4. CONCLUSION

Recent observations indicate that several programs and methods could be effective options for studying computerized structural behavior, such as the ABAQUS software package and the 3D version of Plaxis. This demonstrates that computational modeling is a fundamental resource for the design of structural environments using reference data. Therefore, it is very useful to apply reliable and efficient solutions following a systematic approach, which facilitates obtaining meaningful results for decision-making. Ultimately, the findings of this study offer a viable alternative regarding the scope of geogrid reinforcement (Terramesh® system) through a practical case study of a reinforced soil wall. This was demonstrated by using Plaxis 2D software to describe, estimate, and compare structural behavior in static, dynamic, and simulated environments. However, while the geogrid system is very useful for securing structures erected on compromised soils, other methods may be more effective, such as chemical treatment, geotextile layers, and reinforced concrete. However, the modeling used in this study met initial expectations.

FUNDING INFORMATION

Authors state no funding involved.

AUTHOR CONTRIBUTIONS STATEMENT

This journal uses the Contributor Roles Taxonomy (CRediT) to recognize individual author contributions, reduce authorship disputes, and facilitate collaboration.

Name of Author	C	M	So	Va	Fo	I	R	D	O	E	Vi	Su	P	Fu
Reynaldo Melquiades Reyes Roque	✓	✓	✓	✓	✓	✓	✓	✓	✓	✓		✓	✓	
Lincoln Jimmy	✓	✓	✓	✓	✓	✓	✓	✓	✓	✓				
Fernández Menacho														
Brayanm Reynaldo	✓	✓		✓	✓	✓	✓		✓	✓	✓			
Reyes Huerta														
Fabrizio del Carpio	✓	✓			✓	✓	✓		✓	✓				
Delgado														

C : **C**onceptualization

M : **M**ethodology

So : **S**oftware

Va : **V**alidation

Fo : **F**ormal analysis

I : **I**nvestigation

R : **R**esources

D : **D**ata Curation

O : **O**riginal Draft

E : **E**diting

Vi : **V**isualization

Su : **S**upervision

P : **P**roject administration

Fu : **F**unding acquisition

CONFLICT OF INTEREST STATEMENT

Authors state no conflict of interest.

DATA AVAILABILITY

Derived data supporting the findings of this study are available from the corresponding author [RMRR] on request.





REFERENCES

- [1] M. A. Abdulaziz, M. J. Hamood, and M. Y. Fattah, "A review study on seismic behavior of individual and adjacent structures considering the soil – structure interaction," *Structures*, vol. 52, pp. 348–369, 2023, doi: 10.1016/j.istruc.2023.03.186.
- [2] D. Markulak, T. Dokšanović, I. Radić, and J. Zovkić, "Behaviour of steel frames infilled with environmentally and structurally favourable masonry units," *Engineering Structures*, vol. 204, 2020, doi: 10.1016/j.engstruct.2019.109909.
- [3] W. A. Safi *et al.*, "The structural performance of reinforced concrete members with monolithic non-structural walls under static and dynamic loads," *Buildings*, vol. 10, no. 5, 2020, doi: 10.3390/BUILDINGS10050087.
- [4] R. Resatoglu and S. Jkhsi, "Evaluation of ductility of reinforced concrete structures with shear walls having different thicknesses and different positions," *IIUM Engineering Journal*, vol. 23, no. 2, pp. 32–44, 2022, doi: 10.31436/iiumej.v23i2.2070.
- [5] B. D. Upadhyay, S. S. Sonigra, and S. D. Daxini, "Numerical analysis perspective in structural shape optimization: a review post 2000," *Advances in Engineering Software*, vol. 155, 2021, doi: 10.1016/j.advengsoft.2021.102992.
- [6] K. K.-Frankowska and M. Kulczykowski, "Deformation of model reinforced soil structures: Comparison of theoretical and experimental results," *Geotextiles and Geomembranes*, vol. 49, no. 5, pp. 1176–1191, 2021, doi: 10.1016/j.geotexmem.2021.03.011.
- [7] S. M. Hosseini, M. Yekrangnia, M. Shakiba, M. Bazli, and A. V. Oskoue, "Experimental study on seismic performance of squat RC shear walls reinforced with hybrid steel and GFRP rebars," *Structures*, vol. 64, 2024, doi: 10.1016/j.istruc.2024.106487.
- [8] Y. Wang, J. V. Smith, and M. Nazem, "Optimisation of a slope-stabilisation system combining gabion-faced geogrid-reinforced retaining wall with embedded piles," *KSCE Journal of Civil Engineering*, vol. 25, no. 12, pp. 4535–4551, 2021, doi: 10.1007/s12205-021-1300-6.
- [9] C. Costa *et al.*, "Hazardous faults of South America; compilation and overview," *Journal of South American Earth Sciences*, vol. 104, 2020, doi: 10.1016/j.jsames.2020.102837.
- [10] M. Geng, "A short review on the dynamic characteristics of geogrid-reinforced soil retaining walls under cyclic loading," *Advances in Materials Science and Engineering*, vol. 2021, 2021, doi: 10.1155/2021/5537912.
- [11] S. Balaji, S. Vinodh Kumar, and R. G. Ridhuvarsine, "Applications and performance of geogrids in structures," *International Journal of Recent Technology and Engineering*, vol. 8, no. 4, pp. 5495–5500, 2019, doi: 10.35940/ijrte.d8831.118419.
- [12] P. Xu, K. Hatami, and G. Jiang, "Study on seismic stability and performance of reinforced soil walls using shaking table tests," *Geotextiles and Geomembranes*, vol. 48, no. 1, pp. 82–97, 2020, doi: 10.1016/j.geotexmem.2019.103507.
- [13] Y. Lin, S. Liu, B. He, L. Li, and L. Qiao, "Mechanical behavior of geogrid flexible reinforced soil wall subjected to dynamic load," *Buildings*, vol. 14, no. 6, 2024, doi: 10.3390/buildings14061628.
- [14] R. Hamdi, M. Fattah, and M. Aswad, "Studying the settlement of backfill sandy soil behind retaining wall under dynamic loads," *Engineering and Technology Journal*, vol. 38, no. 7, pp. 992–1000, 2020, doi: 10.30684/etj.v38i7a.528.
- [15] A. Johari and M. Maroufi, "System reliability analysis of geogrid reinforced retaining wall using random finite element method," *Transportation Geotechnics*, vol. 48, 2024, doi: 10.1016/j.trgeo.2024.101316.
- [16] Z. Lu, Q. Fan, W. Tian, and J. Li, "Seismic performance analysis of steel frame installed with prefabricated external walls and new connection type," *Journal of Building Engineering*, vol. 84, 2024, doi: 10.1016/j.job.2024.108471.
- [17] M. Akbar, P. Huali, O. Guoqiang, M. U. Arshid, B. Ahmad, and T. Umar, "Investigation of the displacement-based seismic performance of geogrid earth-retaining walls using three-dimensional finite element modeling," *Results in Engineering*, vol. 21, 2024, doi: 10.1016/j.rineng.2024.101802.
- [18] J. Schueller, F. K. Aschenberger, and J. Lane, "Research in transnational higher education: mixed methods, mixed locations, and mixed assumptions," *Innovative Higher Education*, 2024, doi: 10.1007/s10755-024-09726-4.
- [19] M. K. Alam, "A systematic qualitative case study: questions, data collection, NVivo analysis and saturation," *Qualitative Research in Organizations and Management: An International Journal*, vol. 16, no. 1, pp. 1–31, 2021, doi: 10.1108/QROM-09-2019-1825.
- [20] O. Nwabuko, "An overview of research study designs in quantitative research methodology," *American Journal of Medical and Clinical Research and Reviews*, vol. 3, no. 5, pp. 1–6, 2024, doi: 10.58372/2835-6276.1169.
- [21] I. O. Pappas and A. G. Woodside, "Fuzzy-set qualitative comparative analysis (fsQCA): Guidelines for research practice in information systems and marketing," *International Journal of Information Management*, vol. 58, 2021, doi: 10.1016/j.ijinfomgt.2021.102310.
- [22] H. Taherdoost, "Data collection methods and tools for research; a step-by-step guide to choose data collection technique for academic and business research projects," *International Journal of Academic Research in Management*, vol. 10, no. 1, pp. 10–38, 2021.
- [23] R. Q. Ccoyllo, M. A. D. Figueroa, J. D. J. d. Aguila, and I. A. I. Flores, "Evaluation of structural health monitoring at the Edgardo Rebagliati Martins Hospital with a limited number of accelerometers in the city of Lima (in Spanish: *evaluación del monitoreo de la salud estructural en el hospital Edgardo Rebagliati Martins con un número limitado de acelerómetros en la ciudad de Lima*)," *Tecnia*, vol. 32, no. 2, pp. 76–88, 2022, doi: 10.21754/tecnia.v32i2.1422.
- [24] R. M. S. A.-Ne'aimi and H. K. Nasir, "Numerical study of design parameters influencing anchored diaphragm walls for deep excavation," *Innovative Infrastructure Solutions*, vol. 8, no. 11, 2023, doi: 10.1007/s41062-023-01261-z.
- [25] S. Mansouri, D. P. N. Kontoni, and M. Pouraminian, "The effects of the duration, intensity and magnitude of far-fault earthquakes on the seismic response of RC bridges retrofitted with seismic bearings," *Advances in Bridge Engineering*, vol. 3, no. 1, 2022, doi: 10.1186/s43251-022-00069-8.
- [26] A. Paredes, J. Céspedes, and A. Ruiz-Pico, "Evaluation of the seismic performance of an educational institution using nonlinear dynamic analysis," *Revista Ingeniería de Construcción*, vol. 39, no. 2, pp. 219–238, 2024, doi: 10.7764/RIC.00105.21.
- [27] P. Wen, K. Ji, and R. Wen, "Simplified procedure for simulating artificial non-stationary multi-point earthquake accelerograms," *Soil Dynamics and Earthquake Engineering*, vol. 156, 2022, doi: 10.1016/j.soildyn.2022.107239.
- [28] M. Mercuri, M. Pathirage, A. Gregori, and G. Cusatis, "Computational modeling of the out-of-plane behavior of unreinforced irregular masonry," *Engineering Structures*, vol. 223, 2020, doi: 10.1016/j.engstruct.2020.111181.
- [29] S. Cattari, D. Camilletti, A. M. D'Altri, and S. Lagomarsino, "On the use of continuum finite element and equivalent frame models for the seismic assessment of masonry walls," *Journal of Building Engineering*, vol. 43, 2021, doi: 10.1016/j.job.2021.102519.





- [30] N. Ayoub, J. F. Deü, W. Larbi, J. Pais, and L. Rouleau, "Application of the POD method to nonlinear dynamic analysis of reinforced concrete frame structures subjected to earthquakes," *Engineering Structures*, vol. 270, 2022, doi: 10.1016/j.engstruct.2022.114854.
- [31] C. C. Çadır, M. Vekli, and F. Şahinkaya, "Numerical analysis of a finite slope improved with stone columns under the effect of earthquake force," *Natural Hazards*, vol. 106, no. 1, pp. 173–211, 2021, doi: 10.1007/s11069-020-04456-0.
- [32] A. Lees and M. Dobie, "Finite element modeling of a mechanically stabilized earth trial wall," *Transportation Research Record*, vol. 2675, no. 10, pp. 1373–1383, 2021, doi: 10.1177/03611981211016456.
- [33] K. Xia, C. Chen, K. Yang, H. Zhang, and H. Pang, "A case study on the characteristics of footwall ground deformation and movement and their mechanisms," *Natural Hazards*, vol. 104, no. 1, pp. 1039–1077, 2020, doi: 10.1007/s11069-020-04204-4.
- [34] L. Lu, S. Ma, Z. Wang, and Y. Zhang, "Experimental study of the performance of geosynthetics-reinforced soil walls under differential settlements," *Geotextiles and Geomembranes*, vol. 49, no. 1, pp. 97–108, 2021, doi: 10.1016/j.geotexmem.2020.09.007.
- [35] R. I. Kalehsar, M. Khodaei, A. N. Dehghan, and N. Najafi, "Numerical modeling of effect of surcharge load on the stability of nailed soil slopes," *Modeling Earth Systems and Environment*, vol. 8, no. 1, pp. 499–510, 2022, doi: 10.1007/s40808-021-01087-7.
- [36] S. Ereiz, I. Duvnjak, and J. F. J.-Alonso, "Review of finite element model updating methods for structural applications," *Structures*, vol. 41, pp. 684–723, 2022, doi: 10.1016/j.istruc.2022.05.041.

BIOGRAPHIES OF AUTHORS







Reynaldo Melquiades Reyes Roque     is a researcher registered in RENACYT-CONCYTEC, Civil Engineer graduated from UNASAM, with two Master's Degrees in Science: one in Geotechnical Engineering from UNI and the other in Water Resources Engineering from UNASAM. He also holds a Ph.D. in Civil Engineering (UNFV), a Ph.D. in Civil Engineering (AIU, USA), a specialization in Earthquake Engineering (UNI), and a postdoctorate in Scientific Research (UNES, Mexico). Currently, he is a professor in undergraduate and graduate programs, as well as Director of the Academic Department of Civil Engineering at UNASAM. National and international lecturer, he has more than 25 years of experience in soil mechanics consulting, seismic geotechnical engineering, and risk management in civil and mining works. He can be contacted at email: rreyesr@unasam.edu.pe.







Lincoln Jimmy Fernández Menacho     is a Civil Engineer from Universidad Nacional Santiago Antúnez de Mayolo (UNASAM), interested in research. He is an independent consultant. His professional experience stands out in key areas of civil engineering, complemented by a deep interest in knowledge generation and the development of innovative solutions in his field. He can be contacted at email: lfernandezm@unasam.edu.pe.



Brayann Reynaldo Reyes Huerta     is an Information Systems Engineer from the Universidad Peruana de Ciencias Aplicadas (UPC), with experience as an independent consultant. He is particularly interested in expanding his research within his area of expertise, contributing with practical approaches and solutions in the field of information systems. He can be contacted at email: U201710223@upc.edu.pe.



Fabrizio del Carpio Delgado     is a Master in Civil Engineering with a mention in Construction Engineering. He has extensive professional experience as an executor, supervisor, and coordinator of contracts in urban and rural sanitation projects, hospital infrastructure, road infrastructure, and hydraulic infrastructure. He works as a teacher and researcher in the areas of geotechnical and earth sciences. Since 2020, he has been an active member of the Latin American Committee of ASTM, Chapter D18 (soils and rocks), Subchapter I. He can be contacted at email: fdelcarpiod@unam.edu.pe.